Leukemia (2014) **28**, 589–599

www.nature.com/leu

ORIGINAL ARTICLE

Insights in dynamic kinome reprogramming as a consequence of MEK inhibition in MLL-rearranged AML

KR Kampen[1], A ter Elst[1], H Mahmud[1], FJG Scherpen[1], SH Diks[1], MP Peppelenbosch[2], V de Haas[3], V Guryev[4] and ESJM de Bont[1]

Single kinase-targeted cancer therapies often failed prolonged responses because cancer cells bypass through alternative routes. In this study, high-throughput kinomic and proteomic approaches enabled to identify aberrant activity profiles in mixed lineage leukemia (MLL)-rearranged acute myeloid leukemia (AML) that defined druggable targets. This approach revealed impaired activity of proteins belonging to the mitogen-activated protein kinase (MAPK) and phosphatidylinositol 3-kinase (PI3K) pathway. Pharmacological druggable MAPK pathway targets tested in primary MLL-rearranged AML included MAPKK1/2 (MEK), cyclic AMP-responsive element-binding protein (CREB) and MAPK8/9 (JNK). MEK inhibition showed to severely decrease MLL-rearranged AML cell survival without showing cytotoxicity in normal controls, whereas inhibition of CREB and JNK failed to exhibit MLL selectivity. Exploring the working mechanism of MEK inhibition, we assessed proteome activity in response to MEK inhibition in THP-1. MAPK1/3 (Erk) phosphorylation was instantly decreased in concurrence with a sustained Akt/mammalian target of rapamycin (mTOR) phosphorylation that enabled a subpopulation of cells to survive MEK inhibition. After exhaustion of MEK inhibition the AML cells recovered via increased activity of vascular endothelial growth factor receptor-2 (VEGFR-2) and Erk proteins to resume their proliferative state. Combined MEK and VEGFR-2 inhibition strengthened the reduction in MLL-rearranged AML cell survival by blocking the Akt/mTOR and MAPK pathways simultaneously. The generation of insights in cancerous altered activity profiles and alternative escape mechanisms upon targeted therapy allows the rational design of novel combination strategies.

Leukemia (2014) **28,** 589–599; doi:10.1038/leu.2013.342

Keywords: AML; MLL; VEGFR-2; KDR

INTRODUCTION

Cancerous cells arise when somatic cells are able to escape the restraints that normally withhold them from unlimited expansion. Cancer progression is thought to be the net result of signaling through various protein-mediated networks driving cell proliferation and survival. The kinome networks can be affected by numerous factors; for example, genetic aberrations, oncogenic-activating mutations, silencing tumor-suppressor mutations, epigenetic modifications and stromal interactions. The translation of these factors affects signaling kinase networks to promote proliferative, anti-apoptotic and metabolic stimuli to induce cancer progression.

Specific deregulated protein activity is frequently observed in leukemia.[1–6] Therapy has adapted to some extent, as kinase inhibitor imatinib reached >90% response rates in chronic myeloid leukemia.[7] Nevertheless, kinase-targeted cancer therapies can default when cancer cells bypass through alternative routes, adaptations in redundancy, and escape mechanisms upon single kinase inhibitor therapy.[8] In order to circumvent the constraints of a certain pharmacological inhibitor, it is desirable to monitor intrinsic fluctuations in cellular pathways found to be essential for cell proliferation and survival to develop the most successful combination therapy approach for disease-specific subgroups. Rational designs of kinase inhibitor or receptor tyrosine kinase (RTK) antibody combinations require a high-throughput measurement of kinome and proteome activity profiles. Dynamic pathway reprogramming and alternative escape routes after the addition of a semi-specific inhibitor seems crucial to design appropriate therapeutic interventions.

Combined high-throughput approaches for kinomic and proteomic profiling determined aberrant kinase profiles in mixed lineage leukemia (MLL)-rearranged acute myeloid leukemia (AML) samples as depicted in the study design (Figure 1a). The altered activated peptide and protein profiles of a comprehensive set of MLL-rearranged AML patient samples allowed the selection of possible druggable mitogen-activated protein kinase (MAPK) pathway targets, that is, MAPKK1/2 (MEK), cyclic AMP-responsive element-binding protein (CREB) and control target MAPK8/9 (JNK). Pharmacological MEK inhibition in MLL-rearranged AML cells resulted in dynamic pathway adaptations, through sustained activation of the Akt/mTOR pathway that permitted a subpopulation of AML cells to survive MEK inhibition, which allowed an extreme increased activity of vascular endothelial growth factor receptor-2 (VEGFR-2) and MAPK1/3 (Erk) signaling proteins after inhibitor exhaustion. The dynamic escape mechanism allowed us to predict and test the efficacy of a novel combination strategy. Combined MEK and VEGFR-2 inhibition induced a more sustained cell death in a subset of MLL-rearranged AML primary samples and in AML cell lines.

[1]Department of Pediatric Oncology/Hematology, Beatrix Children's Hospital, University Medical Center Groningen, University of Groningen, Groningen, The Netherlands; [2]Department of Gastroenterology and Hepatology, Erasmus Medical Center, Rotterdam, The Netherlands; [3]Dutch Childhood Oncology Group, Erasmus University College, Hague, The Netherlands and [4]European Research Institute for the Biology of Ageing, University Medical Center Groningen, University of Groningen, Groningen, The Netherlands. Correspondence: Professor ESJM de Bont, Department of Pediatric Oncology/Hematology, Beatrix Children's Hospital, University Medical Center Groningen, University of Groningen PO Box 30.001, 9700 RB Groningen, The Netherlands.
E-mail: e.s.j.m.de.bont@umcg.nl
Received 16 September 2013; revised 30 October 2013; accepted 7 November 2013; accepted article preview online 18 November 2013; advance online publication, 13 December 2013

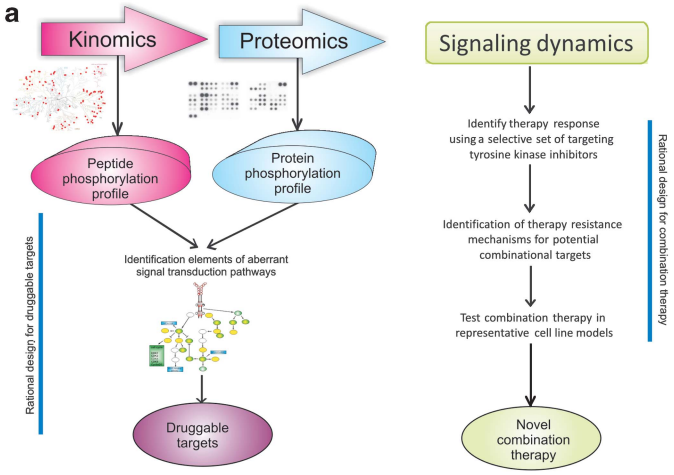

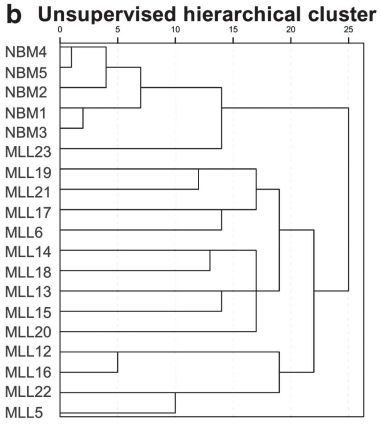

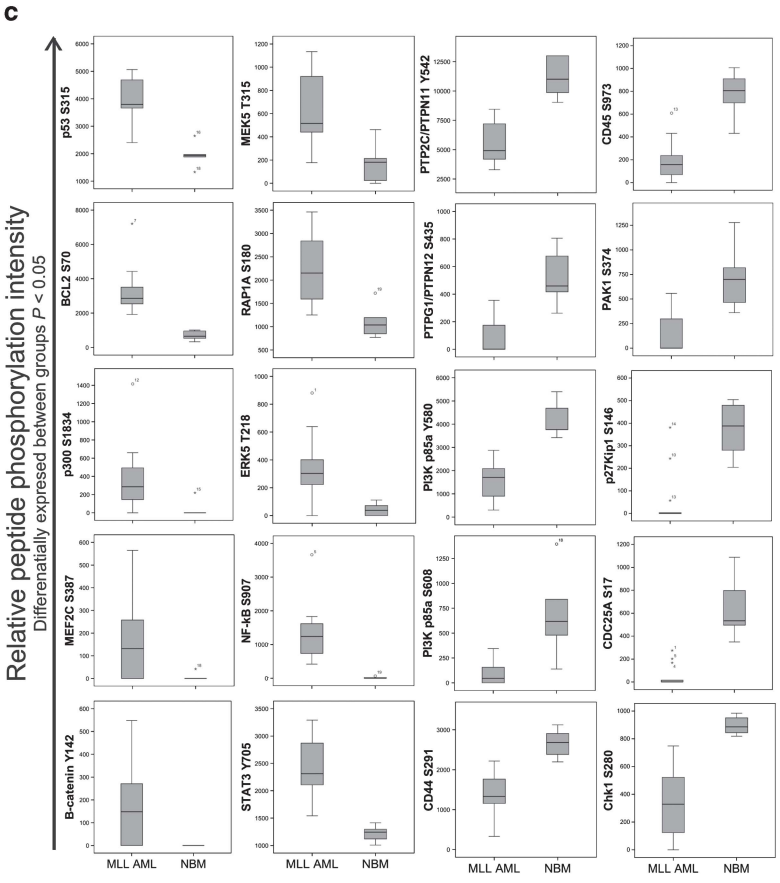

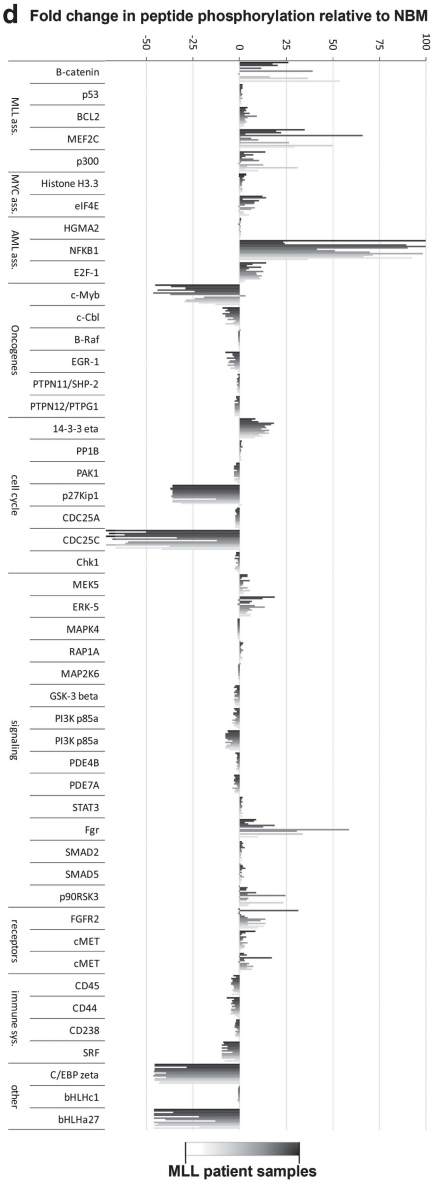

MATERIALS AND METHODS

AML patient samples and cell lines

HL-60, THP-1, MOLM13, OCI AML3, HEL, Kasumi, Hela and DLD-1 cell lines are obtained from American Type Culture Collection (Manassas, VA, USA). THP-1 is characterized by a MLL-AF9 rearrangement and HL60 is characterized by chromosome 5, 9 and 17 abnormalities, both showing additional N-RAS mutations. All cell lines are cultured in RPMI-1640 medium supplemented with 1% penicillin/streptomycin and 10% fetal calf serum (Bodinco, Alkmaar, The Netherlands). After getting written informed consent, the mononuclear cell fraction of bone marrow form healthy controls and pediatric AML patients was obtained and cryopreserved, and approved by the Medical Ethical Committee of the University Medical Center Groningen. Samples were thawed rapidly at 37 °C and diluted in a 6-ml volume of newborn calf serum, as described previously.[9] The remaining AML blast population contained >95% viable cells (Supplementary Figure 1A). MLL-rearranged AML samples contain >95% (±6%) myeloblasts after exclusion of cell debris and subtraction of lymphoid cells determined using flow cytometric analysis. The MLL-rearranged AML sample characteristics are displayed in Supplementary Table 1. Dutch Childhood Oncology Group MLL-rearranged AML patient data on RAS pathway mutations were obtained by the Department of Pediatric Oncology/Hematology, Erasmus MC—Sophia Children's Hospital, Rotterdam, The Netherlands.

Fluorescence-activated cell sorting

Mononuclear cells were blocked by phosphate-buffered saline 1% bovine serum albumin (Sigma-Aldrich, St Louis, MO, USA) and stained with VEGFR-2 antibody (Sigma-Aldrich). VEGFR-2 antibodies were visualized using phycoerythrin-conjugated secondary antibody (DAKO Cytomation, Heverlee, Belgium). IgG1-phycoerythrin and secondary antibody were used as a negative control (Supplementary Figure 1B). Membrane protein expression was measured using LSRII (BD FACS DIVA software, BD Bioscience, Breda, the Netherlands). AML cells were stained with Annexin V-FITC for 15 min in staining buffer following manufacturer's protocol (Annexin-V-FLUOS staining kit, Roche, Woerden, the Netherlands). Apoptotic and viable populations are distinguished based upon Annexin-V expression. The data were analyzed using FlowJo software (Tree Star Inc., Ashland, OR, USA). Expression levels above 2% were considered as actual protein expression, reaching above isotype controls.

Pepchip

Peptide activity profiles of MLL-rearranged AML samples ($n = 14$) and normal bone marrow (NBM) samples ($n = 5$) were determined using the PepChipTM Kinomics microarray system (Pepscan, Lelystad, The Netherlands). The microarrays contain 1024 peptides that are spotted on glass slides in triplicate blocks. The protein-derived peptide sequences contain phosphorylation sites that can be phosphorylated by the sample substrates. Per patient sample, 0.5×10^6 cells were lysed in 100 μl of cell lysis buffer as described previously.[4] Peptide array incubation mix was produced by adding 10 ml of filter-cleared activation mix (50% glycerol, 50 mM (γ-33P) ATP, 0.05% (v/v) Brij-35, 0.25 mg/ml bovine serum albumin, (γ-33P) ATP (1000 kBq)) onto the chip incubated at 37 °C in a humidified stove for 90 min. Subsequently, the peptide array was washed twice with Tris-buffered saline with Tween, twice in 2 M NaCl, twice in demineralized H_2O and then air-dried. Analysis of peptide array: The chips were exposed to a phospho-imager plate for 72 h, signaling intensity of the peptide spots was analyzed using array software (ScanAlyze, Eisen Software, http://rana.lbl.gov/eisen). ATP and batch numbers of the array slides were all identical and all samples were analyzed in one run to minimize methodological variation. Data analysis: After background subtraction, the spot intensities were quantile normalized and negative values were converted to 0.1. A pre-filtering step was realized by Pearson correlation coefficient over the triplicates. Samples were discarded from the analysis when the Pearson's Correlation coefficient of triplicate was below 0.6 (mean 0.89). Medians from the triplicates were used for further analysis. Significant differences between MLL-rearranged AML and NBM were determined using a Mann–Whitney *U* non-parametric test.

Human phospho-proteome arrays

Human phospho-protein antibody array kits were used from R&D systems (Minneapolis, MN, USA), whereas the phospho-RTK arrays were used from Cell Signaling (Boston, MA, USA). Multiple RTKs and proteins were printed in duplicates onto membranes or glass slides to measure protein phosphorylation from sample lysates according to manufacturer's protocol. The phospho-protein kinase intensity spots are visualized by chemiluminescence, on an X-ray film and scanned. Signaling intensity of the proteins was analyzed with array software (ScanAlyze, Eisen Software, http://rana.lbl.gov/eisen). For the phospho-protein antibody arrays (R&D systems), data were interpreted as actual expression when duplicate intensities reached above 500 pixel intensity, standard deviations did not exceed expression intensities and were below 500 pixel intensity. Expression of phosphorylated proteins reached from pixel intensities; 500–25 000. Data normalization was achieved by determining the mean signal over each array. Phospho-protein spot intensities from duplicates were divided by the median array signal per patient sample. Multivariate analysis using a Bonferoni correction for multiple testing defined significant phosphorylated protein changes between experimental groups (MLL-AML, other cytogenetic AML and NBM samples). For the PathScan phospho-RTK array, similar amounts of protein were subjected to the arrays per sample condition, which was realized by upfront evaluation using a bovine serum albumin protein assay (Thermo Scientific, Rockford, IL, USA). For the PathScan phospho-RTK array, all samples were used on one glass array slide, so for these samples' additional normalization was not required.

Western blot

1×10^6 cells were lysed in laemmli sample buffer (Bio-Rad Laboratories, Veenendaal, The Netherlands). Proteins were separated by SDS-polyacrylamide gel electrophoresis, and transported to nitrocellulose membranes. First, the membranes were incubated overnight with monoclonal primary antibodies for p-mTOR, pAkt, t-Akt, pErk, tErk, pSTAT5, tSTAT5, p-CREB, t-CREB, p-RSK, t-RSK, p-JNK and actin (Cell Signaling), and p-p27, t-p27, p-p38, t-p38 (Signalway Antibody, Baltimore, MD, USA), followed by 1 h incubation with HRP-conjugated secondary antibodies (DAKO Cytomation). Protein bands were visualized by chemiluminescence, on an X-ray film and scanned.

Cell survival assays

Quantification of leukemia cell viability was carried out using WST-1 assays for primary samples and cell lines. WST-1 assays were performed in sextuple according to manufacturer's protocol (Roche). AML cells were seeded at a density of $0.1–1 \times 10^5$ cells per 100 μl/well in RPMI medium supplemented with 1–10% fetal calf serum. Compounds: VEGFR-2 blocking antibody (Imclone systems, New York, NY, USA, at concentrations of

Figure 1. Kinome profiling of MLL-rearranged AML reveals active signaling pathways. (**a**) Experimental design for the rational identification of kinase inhibitor combination therapies. Proteome and kinome profiles allows the identification of druggable targets. Tracking cellular changes upon single protein kinase inhibition admit the selection of potential combinational targets for dual kinase inhibition approaches. Survival analysis and protein phosphorylation analysis identified cellular therapy responses throughout this process for the rational design of novel combination therapies. (**b**) This dendrogram shows the unsupervised hierarchical clustering using the Pearson's correlation method between group linkage using *z*-scores. The plot presents unsupervised clustering of MLL-rearranged AML and NBM samples based upon quantile-normalized peptide phosphorylation intensities across 1024 peptides. (**c**) The protein-derived peptide phosphorylation spot intensities defined by the ability of sample lysate substrates to phosphorylate the peptides showed the fold difference in peptide phosphorylation intensity of each individual MLL-rearranged AML, which is set against the mean for NBM samples ($n = 5$). This plot presents fold differences for a selective group of interesting categorized peptides. Proteins from which the peptide sequences are derived are indicated. (**d**) Box-plots show the variation in phosphorylation intensities of selected protein-derived peptides between MLL-rearranged AML samples and NBM controls. Presented are the proteins from which the peptide sequences are derived and the explicit peptide phosphorylation sites are indicated.

250 ng/ml) and/or the MEK inhibitor U0126 (Promega, Madison, WI, USA), CREB-1 inhibitor KG-501 (Sigma-Aldrich), JNK II inhibitor in solution (Calbiochem, Merck, Darmstadt, Germany) at different concentrations (1–50 μM). Mitochondrial activity of AML cell was measured after 48 h using a microplate reader at 450 nm (Benchmark; Bio-Rad Laboratories). Cell survival percentages are determined relative to dimethyl sulfoxide-treated cells.

Statistics

Means and their corresponding standard deviations are presented; WST-assays are performed in sixfold, reverse transcription-PCRs are performed in triplicates on one plate, apoptosis analysis using flow cytometric analysis are performed in three independent experiments, phospho-proteome analysis is presented from duplicate spots, unless indicated differently. Unpaired, two-tailed Student's *t*-tests were used for all analysis comparing at least triplicates of two experimental groups, except when described differently.

RESULTS

Kinome profiling identified aberrant peptide activity profiles in MLL-rearranged AML

Figure 1a presents the overall study design. Analysis started out exploring aberrant kinome activity in MLL-rearranged AML samples ($n=14$) as compared with NBM controls ($n=5$) using peptide arrays to identify druggable targets. The peptide arrays allowed unbiased insights into altered kinome signaling activity in MLL-rearranged AML samples. Kinome activity throughout 1024 peptides showed that MLL-rearranged AML samples clustered separately from NBM samples in unsupervised hierarchical cluster analysis (Figure 1b). Cluster analysis clearly displayed how heterogeneous the MLL-rearranged AML subgroup is compared with the densely clustered NBM controls. Next, we defined significantly differential phosphorylated peptides between MLL-rearranged AML samples and NBM controls that are depicted in Supplementary Table 2. Interesting peptides are categorized and highlighted in Figure 1c. As expected, MLL-associated peptide phosphorylation of β-catenin, p53, BCL2, MEF2C and p300 was found to be enhanced in MLL-rearranged AML as compared with NBM. MYC-associated peptide activity of Histone H3.3 and eIF4E was also increased in MLL-rearranged AML patient samples. General AML-associated peptides NF-κβ, HGMA2 and E2-F1 were highly phosphorylated in MLL-rearranged AML samples relative to NBM. Moreover, oncogene-related peptide activity of c-Myb, c-Cbl, B-Raf, EGR-1, SHP-2 and PTPG1 showed to be commonly down-regulated in MLL-rearranged AML samples as compared with NBM. Interestingly, we found decreased peptide activity of DNA damage control and cell cycle regulators Chk-1, CDC25 and p27Kip1 that showed a strong difference in absolute peptide phosphorylation intensities between MLL-rearranged AML as compared with NBM (Figure 1d) in coexistence with an increase in 14-3-3 eta and PP1B peptide activity. As expected, the immune system-related peptides were decreasingly phosphorylated in MLL-rearranged AML samples as compared with NBM. Signaling receptors FGFR2 and cMET were particularly active in MLL-rearranged AML. Focusing on major signaling pathways, several MAPK peptides were higher phosphorylated in MLL-rearranged AML as compared with NBM. Unexpected was the decreased activity of PI3K, p85a and GSK-3 beta peptides that was previously described to be associated with the MLL complex. Other signaling pathway peptides increasingly activated in MLL-rearranged AML included Fgr, STAT3 and p90RSK3. In summary, using peptide array activity profiling, we showed impaired activity of PI3K and MAPK signaling pathways and disrupted regulation of the cell cycle and immune responses in MLL-rearranged AML samples as compared with NBM samples. The peptide array results defined MLL-rearranged AML-enriched kinome activity of several pathways that allows to select for potential druggable targets Erk, MEK, p90RSK, BCL2, β-catenin, p300, MEF2, 14-3-3, NF-κβ and Fgr.

Proteome profiling identified aberrant protein activity profiles in MLL-rearranged AML

Complementary to the kinome array results, we gained insights in the activated proteome profile of MLL-rearranged AML samples as compared with NBM. Phospho-proteome arrays allowed quantitative proteome profiling of phosphorylated proteins in individual MLL-rearranged AML ($n=9$) and NBM samples ($n=4$; Figure 2a and Supplementary Table 3). A common increase in phospho-protein expression was found for Akt (S473), CREB (S133), Fgr (Y412), GSK3 (S21/S9), HSP27 (S78/S82), Lck (Y394), Lyn (Y397), $MEK_{1/2}$ (S218/S222/S226), p38 (T180/Y182), RSK (S221), STAT1 (Y701), STAT3 (Y705), STAT5b (Y699) and p53 (S392) phosphorylation in MLL-rearranged AML samples as compared with NBM (Figure 2a, Akt $P=0.005$, CREB $P=0.005$, Fgr $P=0.015$, GSK3 $P=0.031$, HSP27 $P=0.031$, Lck $P=0.005$, Lyn $P=0.005$, MEK $P=0.021$, p38 $P=0.005$, RSK $P=0.005$, STAT1 $P=0.005$, STAT3; $P=0.015$, STAT5b $P=0.025$ and p53 $P=0.005$). Phospho-protein expression downregulated in MLL-rearranged AML as compared with NBM included AMPK2a (T172), Hck (Y411), MSK (S376/S360), Src (Y419), STAT2 (Y689), STAT4 (Y693), p70S6k (T229/T241/T424) and mTOR (S2448) (AMPK2a $P=0.005$, Hck $P=0.005$, MSK $P=0.014$, Src $P=0.021$, STAT2 $P=0.005$, STAT4 $P=0.031$, p70S6k $P=0.009$ and $P=0.005$ and mTOR $P=0.005$).

MLL selectivity was defined using AML samples ($n=5$) that have no MLL rearrangement. The common overlap in abnormal activity of proteins in all AML samples as compared with NBM included the increased phosphorylation of STAT1, GSK-3, p53 and the decreased phosphorylation of Src (Figure 2b). Selective decreased protein phosphorylation was found for AMPK2a, p70S6k, mTOR, STAT2 and MSK in MLL-rearranged AML samples as compared with non-MLL-rearranged AML and NBM samples (Figure 2b, AMPK2a $P<0.001$, p70S6k $P<0.001$ and $P=0.002$, mTOR $P=0.001$, STAT2 $P=0.013$ and MSK $P=0.029$). Most importantly, we found selective increased phospho-protein expression of Akt (S473), CREB, Fgr, Lck, Lyn, p38, RSK (S221), STAT3 and MEK in MLL-rearranged AML as compared with non-MLL-rearranged AML and NBM (Figure 2b, Akt $P<0.001$, CREB $P<0.001$, p38 $P<0.001$, RSK $P<0.001$, STAT3 $P=0.027$, and MEK $P=0.043$). The accuracy of differences in protein phosphorylation can be appreciated from the presented membranes (Figure 2c).

The integration of kinome and proteome profiles identified a complementary overlap in altered signaling pathways including an increased activity of the MAPK pathway and an impaired activity of the PI3K pathway in co-occurrence with pro-survival activity. Our rational design for drug target discovery identified MEK, RSK, CREB, BCL2, p38, STAT3, Fgr, NF-κβ, β-catenin and p300 as MLL-rearranged AML potential therapeutic targets.

Selectivity for MLL-rearranged AML cell death upon MEK inhibition

MLL-rearranged AML kinome and proteome profiles identified increased activity of the MAPK signaling pathway in MLL-rearranged AML primary samples. MEK and CREB were further investigated for therapeutic applicability in MLL-rearranged AML blasts together with non-selective target control JNK.

MEK inhibitor U0126 effectively reduced the cell survival of primary MLL-rearranged AML samples in contrast to NBM cells that proved to be resistant to the U0126 MEK inhibition (mean $LC50=3.5\pm1.7$ μM in primary MLL-rearranged AML and $LC50>50$ μM for NBM, Figure 3a). Selectivity was further evaluated using AML samples ($n=5$) that have no MLL rearrangement. The MLL-rearranged AML samples were found most sensitive to MEK inhibition compared with NBM and other karyotype AMLs (10 μM, $P=0.015$; 20 μM, $P=0.012$, Figure 3b). Second, CREB-1 was

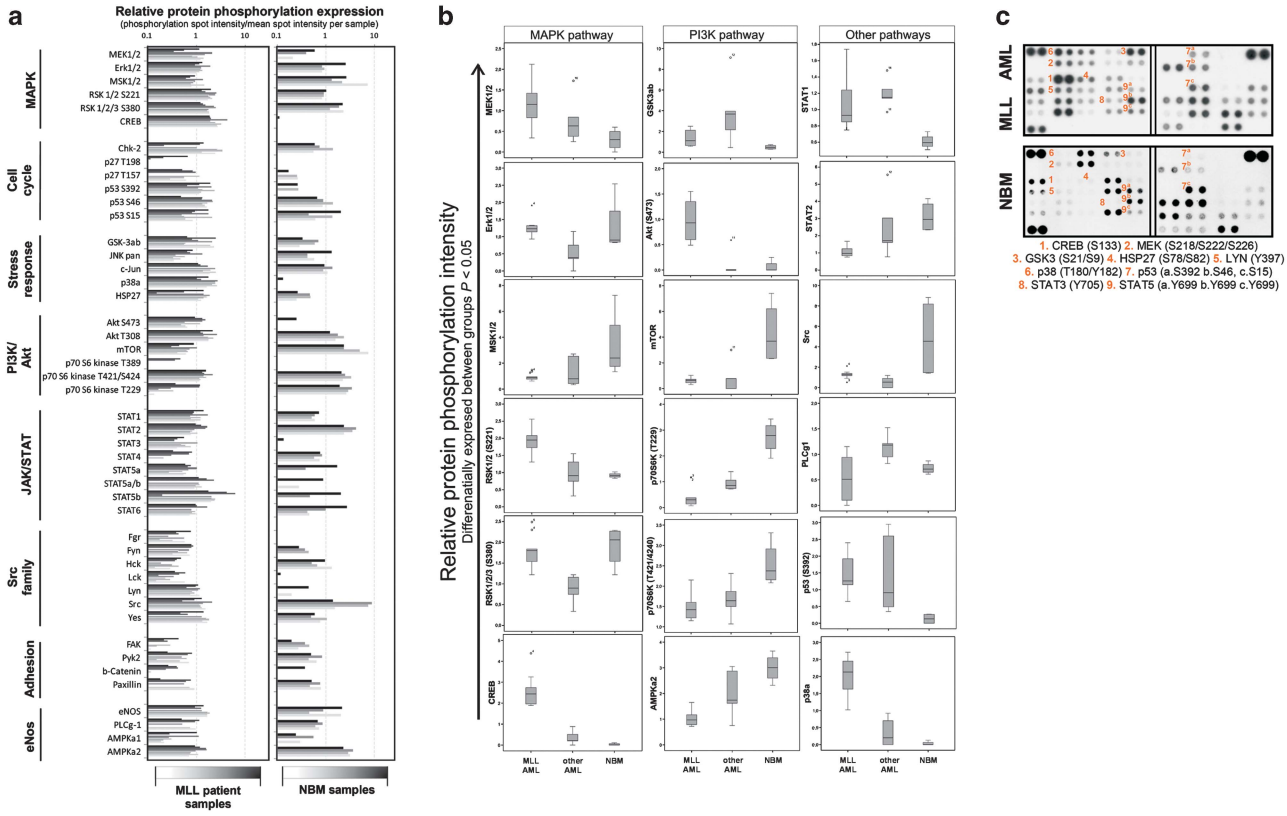

Figure 2. MLL-rearranged AML selective phospho-proteome profiles as compared with non-MLL-AML and NBM. (**a**) Phospho-proteome analysis of nine individual MLL-rearranged AML patient samples and four individual NBM samples. The plot displayed the phosphorylation sites of the proteins present on the proteome array that are categorized upon different signal transduction pathways. (**b**) Significant differentially expressed phosphorylated proteins were shown in box-plots for MLL-rearranged AML patient samples ($n = 9$), non-MLL-rearranged AML samples ($n = 5$) and NBM samples ($n = 4$). Box-plots show a selection of phospho-proteins with high expression intensities and were categorized upon corresponding signaling pathway. (**c**) Representative phospho-proteome array membranes display the variance in protein phosphorylation intensities on the array membranes between MLL-rearranged AML and NBM.

targeted using KG-501 that inhibits the CREB/CBP interaction. CREB showed to induce AML cell death effectively in one MLL-rearranged AML sample, however, overall we found an insufficient cellular response of primary MLL-rearranged AML samples and NBM cells (Figure 3c). For JNK inhibition, we used the JNK II inhibitor. Inhibition of JNK decreased the cell survival of MLL-rearranged AML samples and NBM cells solely at high dosage. As anticipated, JNK inhibition was not found to be selective for MLL-rearranged AML (Figure 3d). Of these three targets, pharmacological MEK inhibition was shown to decrease MLL-rearranged AML cells survival most efficiently without inducing cytotoxicity in NBM cells. MEK inhibition sufficiently targeted MEK in the MLL-rearranged AML patient samples as was shown by decreased downstream Erk phosphorylation levels (Supplementary Figure 2).

Next, we investigated the operability of an AML cell line model to gain more insights into MEK inhibition. We analyzed MEK inhibition in three N-RAS mutant and three RAS wild-type AML cell lines (Figure 3e, LC50 = 3 ± 2 μM and 14 ± 3.4 μM). We found that THP-1 (monocytic) MLL-rearranged AML cell line sensitivity to the MEK inhibitor was most analog with primary MLL-rearranged AML samples. As a competitor non-MLL-arranged AML cell line, we have chosen the HL60 (myelomonocytic) AML cell line that showed to overlap in inhibitor sensitivity and also harbors a N-RAS mutation. Immunoblots of the two AML cell lines confirmed the utility of AML competitor cell line HL60 as it mainly represents a similar phosphorylation profile as THP-1. We found an overlap in phosphorylation levels of proteins: Erk, CREB, p27, p38, and JNK (Figure 3f). Although MEK inhibition was comparable between the two cell lines, THP-1 was more responsive to CREB inhibition and JNK inhibition (Figure 3g). All therapeutics were shown to effectively inhibit the target of interest, by reducing the phosphorylation of Erk upon MEK inhibition, reducing the phosphorylation of JNK upon JNK inhibition, and through down modulation of BCL2 downstream of CREB upon CREB inhibition (Figure 3h). These cell line models were further evaluated for MEK inhibition downstream signaling effects.

Sustained Akt/mTOR pathway activation in response to MEK inhibition: a resistance pathway

In vitro data in AML patient samples previously showed severely decreased cell viability upon MEK inhibition, whereas in a phase II clinical trial MEK inhibition only resulted in non-sustained responses, suggestive for revelation of (ab)normal feedback mechanisms.[10,11] Single MEK inhibition has previously been shown to promote therapeutic resistance by c-Myc degradation leading to the reprogrammed RTK response in triple-negative breast cancer.[8]

Pharmacological MEK inhibition in THP-1 decreased the AML cell survival through growth inhibition and apoptosis inducing mechanisms without reaching cytotoxicity levels, as determined in negative controls (Figures 4a–c). MEK inhibition was shown to target MLL-rearranged cells at a concentration of 5 μM, demonstrating optimal settings to recognize early signs of therapeutic resistance. Using immunoblot analysis, we found that 24 h MEK inhibition reduced Erk phosphorylation and simultaneously increased Akt^{S473} phosphorylation (Figure 4d). As a next step, we investigated a possible MEK-induced therapeutic failure

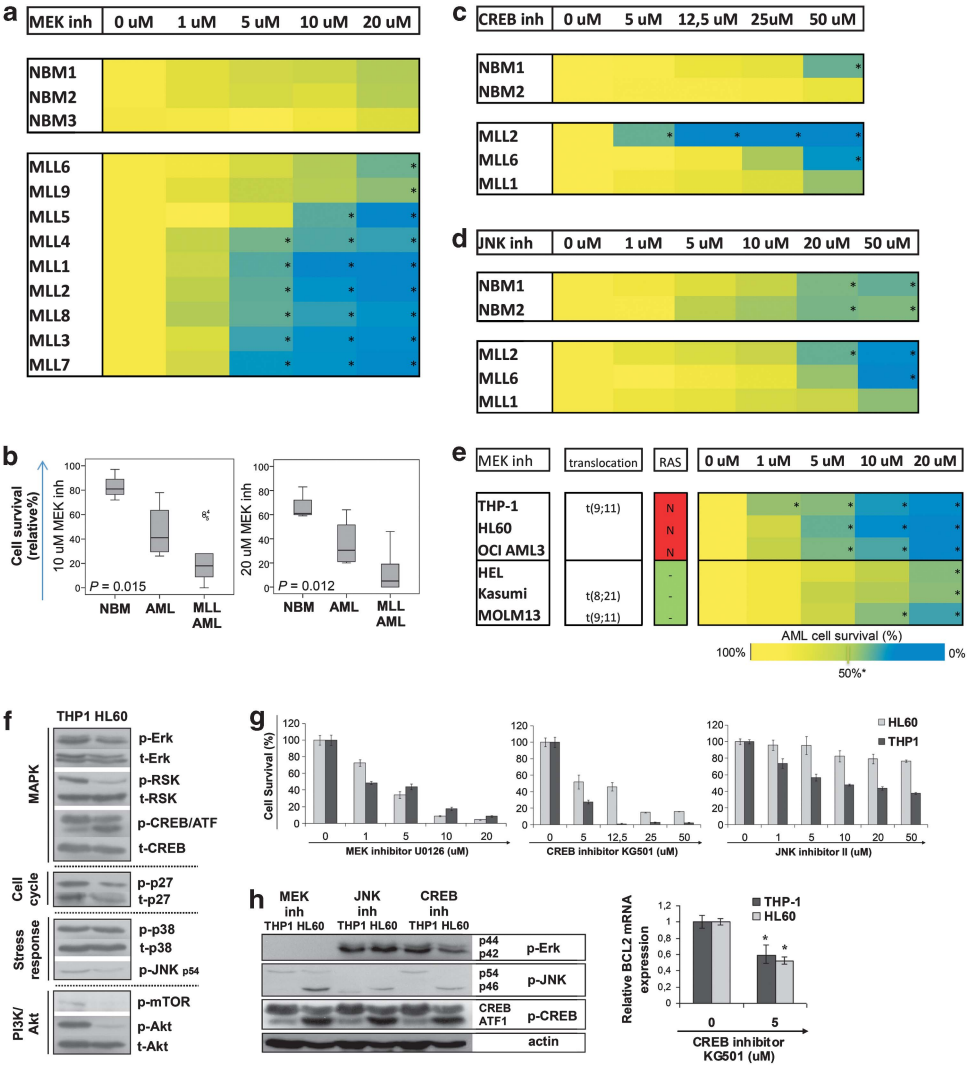

Figure 3. MEK showed most suitable to induce MLL-rearranged AML cell death. (**a**) WST-1 cell survival assay analysis in three NBM controls and nine primary MLL-rearranged AML patient samples upon different concentrations of MEK inhibitor (0/1/5/10/20 μM) showed an MLL rearrangement-selective MEK inhibition induced cell death after 48 h treatment. (**b**) Box-plots present the cell survival percentages between MLL-rearranged AML ($n = 9$), non-MLL-rearranged AML ($n = 5$) and NBM ($n = 3$) samples using 10 and 20 μM MEK inhibitor treatment for 48 h. (**c**) WST-1 cell survival assay analysis in two NBM controls and three primary MLL-rearranged AML patient samples using different concentrations of CREB inhibitor (0/5/12.5/25/50 μM) induced MLL-rearranged AML cell death solely in one patient sample after 48 h of treatment. (**d**) WST-1 cell survival assay analysis in two NBM controls and three primary MLL-rearranged AML patient samples using the JNK-II inhibitor in different concentrations (0/1/5/10/20/50 μM) showed a limiting capacity to induce cell death in MLL-rearranged AML and NBM samples after 48 h treatment. (**e**) WST-1 cell survival analysis upon MEK inhibition in a panel of N-RAS mutant (N) and wild-type (-) AML cell lines showed the susceptibility of N-RAS mutant and wild-type AML cell lines to different concentrations of MEK inhibition (0/1/5/10/20 μM) after 48 h treatment. (**f**) Immunoblots showing the variation in phosphorylation levels of Erk, RSK, CREB p27, p38, JNK, mTOR and Akt protein kinases between the MLL-rearranged AML THP-1 cells and non-MLL-rearranged AML cell line HL60. (**g**) MEK, JNK and CREB inhibition in AML cell lines presenting the dose-dependent effect on the AML cell survival in two independent cell lines; MLL-rearranged AML cell line THP-1 and non-MLL-rearranged AML cell line HL60 after 48 h treatment. (**h**) The efficiency of MEK, JNK and CREB inhibition was evaluated by immunoblots of phosphorylated Erk, JNK and CREB after 48 h treatment. The CREB inhibitor KG-501 blocks the formation of a CREB-binding protein complex on which downstream BCL2 activation is partly dependent. Quantitative reverse transcription-PCR analysis showed that BCL2 was reduced by 50% upon 24 h CREB inhibition. *LC50, a more than 50% reduction in cell survival.

through alternative routes by a broader screening method using phospho-proteome array analysis. The phospho-RTK array analysis of THP-1 showed pronounced levels of Akt^{S473}, Erk, Lck, p70S6k, Src and VEGFR-2 phosphorylation that changed upon MEK inhibition. The 24 h and 48 h short-term responses mainly resulted in a decrease in the phosphorylation of Erk and p70S6 (Figures 4e and f). Similar as we found with immunoblot analysis, Akt^{S473} phosphorylation was increased upon MEK inhibition at 24 h. Long-term MEK inhibition was exhausted at day 5, which allowed an extreme induction in phosphorylation of Erk and VEGFR-2 to recover from the MEK inhibition. P70S6 kinase was not re-activated, but Akt levels were reduced back to normal levels. In line with the phospho-proteomic arrays, immunoblots confirmed the short-term inhibition of MAPK proteins and their re-activation after 72 h, which allowed to recover from MEK inhibition (Figure 4g). Interestingly, mTOR phosphorylation remained activated during MEK inhibition, demonstrating a typical cellular resistance pattern. These data indicate that MEK inhibitor resistance is facilitated via the Akt/mTOR pathway that enables a subpopulation of AML cells to survive MEK inhibition and recover via co-activation of VEGFR-2 and Erk.

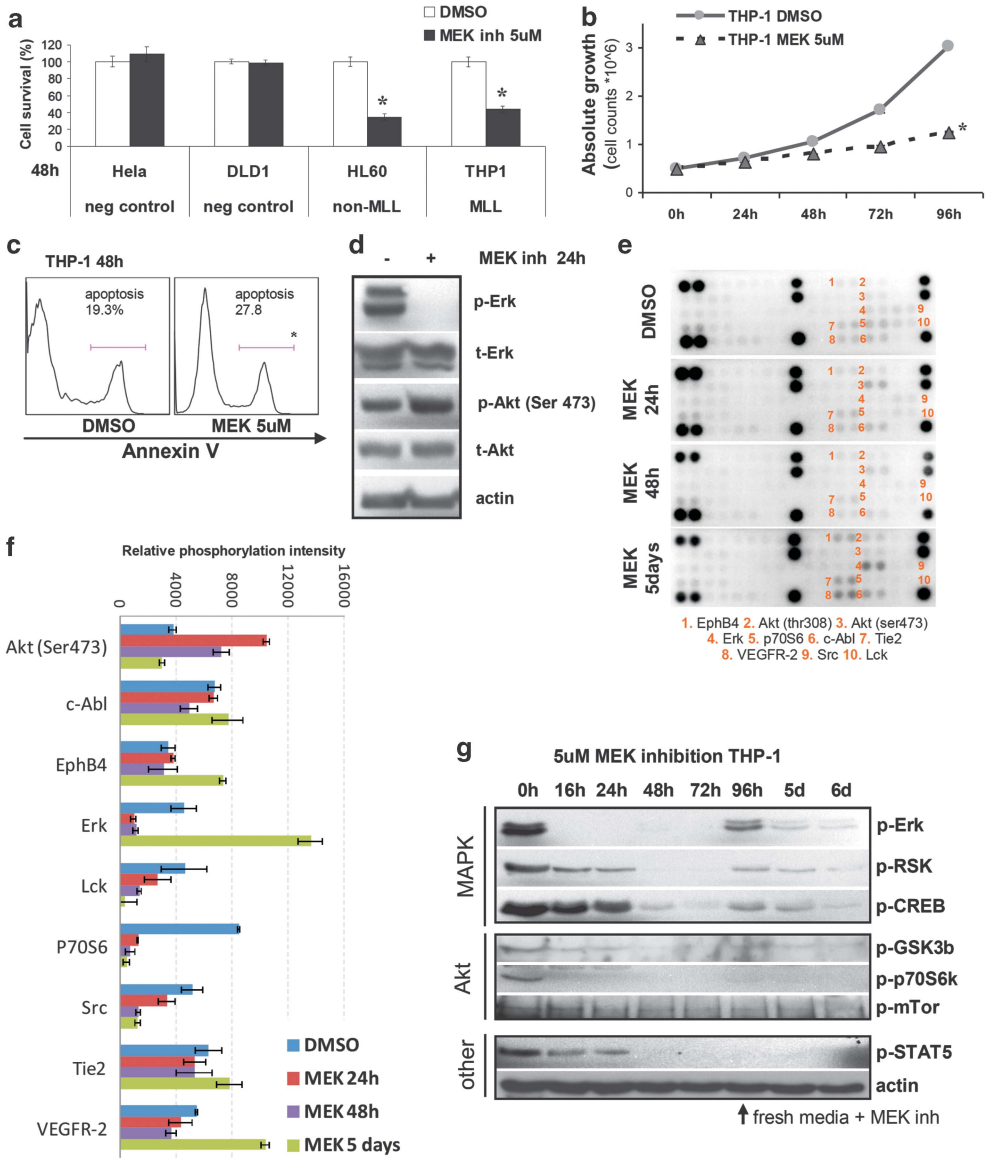

Figure 4. Long-term MEK inhibition induced resistance. (**a**) WST-1 cell survival assay analysis using 5 μM MEK inhibitor in AML cell lines and non-responsive control cell lines. MEK inhibition significantly reduced AML cell survival at 5 μM without reaching cytotoxicity levels as determined in Hela and DLD1 cell lines. (**b**) Growth evaluation by absolute cell counts showed that MEK inhibition significantly reduced the absolute growth of THP-1 MLL-rearranged AML cells in contrast to the dimethyl sulfoxide (DMSO)-treated control cells after 4 days. (**c**) Annexin V flow cytometric apoptosis analysis displayed an induction in Annexin V-positive cells upon 5 μM MEK inhibition in MLL-rearranged THP-1 cells after 48 h treatment. (**d**) Immunoblot analysis of phosphorylated and total protein levels for Erk and Akt upon 24 h using 5 μM MEK inhibition in THP-1 cells. Downregulation of protein expression and phosphorylation was not due to an overall increase in protein synthesis, as shown with western blot analysis against actin. (**e**) Phospho-proteome arrays of THP-1 cells treated with 5 μM MEK inhibition, showing the time-dependent MEK inhibitory effects after 24 h, 48 h and 5 days of treatment. The phospho-proteins that showed the most robust changes in phosphorylation are indicated by numbers that are explained underneath the membranes. (**f**) Quantification of the phospho-proteome arrays were presented in a bar-graph with error-bars of duplicate spots that displayed the time-dependent MEK inhibitory effects after 24 h, 48 h and 5 days of treatment. (**g**) Immunoblots confirmation of the proteome array results showed that Erk was re-activated after 96 h. Thereafter, a second dosage of MEK inhibitor was added to the AML cell culture, as indicated by the arrow. Phosphorylation of p70S6 kinase was reduced and not re-activated. RSK and CREB phosphorylation patterns were comparable to the Erk activation pattern. Phosphorylation of mTOR was shortly decreased after 24 h and remained activated. *Significant differences between two individual groups, Student's *t*-test, $P < 0.05$.

Novel combination therapy promotes MLL-rearranged AML cell death through simultaneous inhibition of MEK and VEGFR-2

MEK-targeted therapeutic failure is a common resistance consequence of cellular intrinsic evolution through alternative routes of protein signaling pathway activation, suggesting the need to target multiple activated pathways. To meet this challenge, we investigated the compatibility of combined MEK and VEGFR-2 inhibition to overcome therapeutic resistance and recovery by induced phosphorylation of the Akt/mTOR survival pathway and the maintenance of Erk and VEGFR-2 signaling protein activity. First, we investigated the functionality of VEGFR-2 antibody therapy in THP-1, which showed to sufficiently block VEGFR-2 membrane expression (Figure 5a). Next, we analyzed short-term combination therapy effects on the AML cell survival. Combination

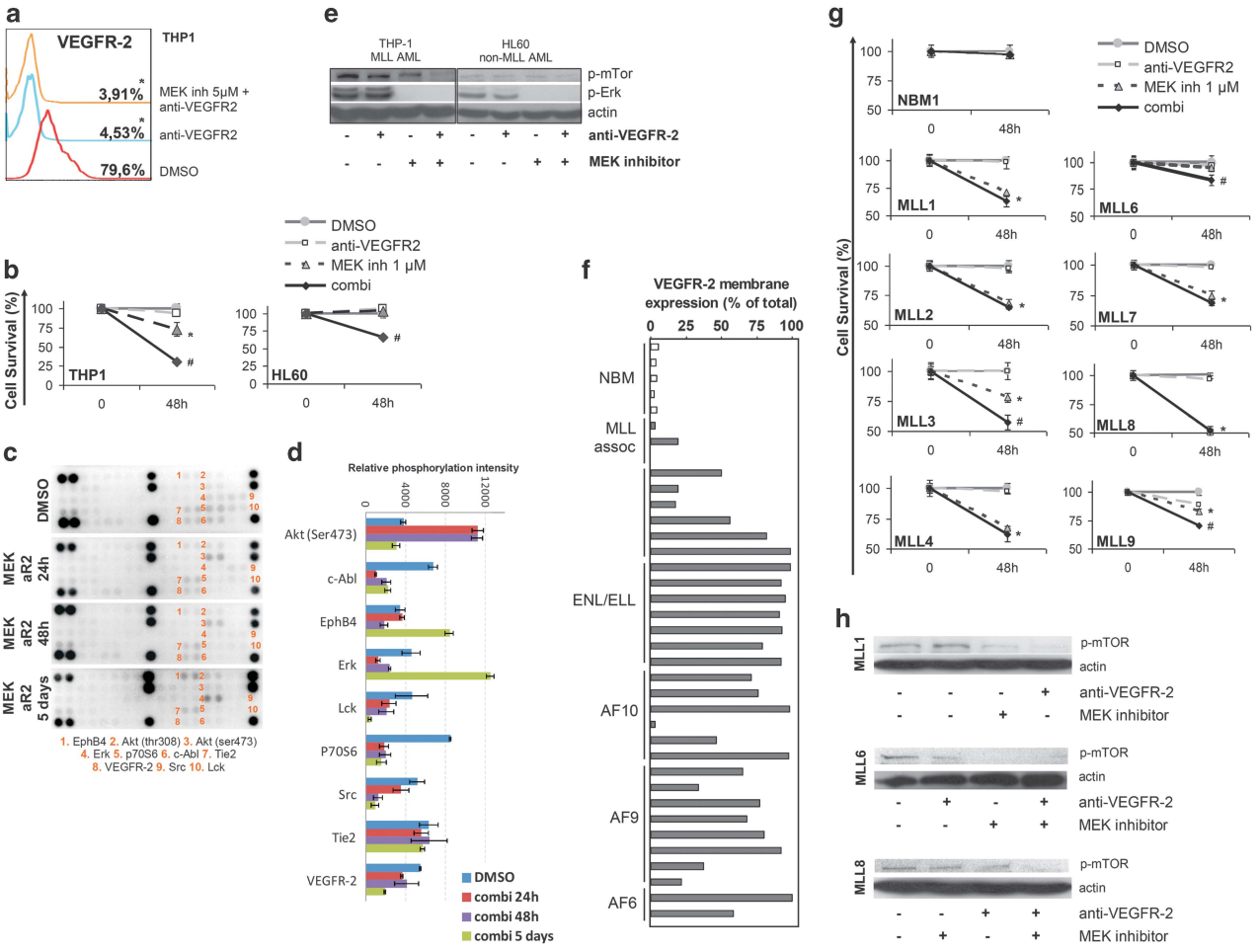

Figure 5. Combined MEK and VEGFR-2 inhibition decreased MLL-rearranged AML cell survival by blocking the activity of both the MAPK and the PI3K/Akt pathway. (**a**) Flow cytometric analysis of VEGFR-2 membrane protein expression levels in untreated control cells and upon VEGFR-2-blocking antibody therapy (250 ng/ml) and combined VEGFR-2 and MEK (5 μM) inhibition. (**b**) Cell survival analysis of single or combined VEGFR-2 (250 ng/ml) and MEK (1 μM) inhibition synergistically induced cell death in the MLL-rearranged AML cell line THP-1 and non-MLL-rearranged AML cell line HL60. (**c**) Phospho-proteome arrays show the combined MEK (5 μM) and VEGFR-2 (250 ng/ml) inhibitory effects in THP-1 after 24 h, 48 h and 5 days of treatment. The phospho-proteins that showed the most robust changes in phosphorylation are indicated by numbers that are explained underneath the membranes. (**d**) Quantification of the phospho-proteome arrays after 24 h, 48 h and 5 days of combination treatment was presented in a bar graph with error bars of duplicate spots. (**e**) Immunoblot analysis of phosphorylated Erk and mTOR using single or combined VEGFR-2 (250 ng/ml) and MEK (5 μM) inhibition in THP-1 and HL60 after 24 h treatment. Changes in protein phosphorylation were not due to an overall increase in protein synthesis, as shown with western blot analysis against actin. (**f**) Flow cytometric analysis of VEGFR-2 membrane protein expression levels in a large panel of NBM controls (white bars) and MLL-rearranged AML patient samples (gray bars). VEGFR-2 membrane protein expression is presented as the percentage of viable blasts that express VEGFR-2 on their cell membrane relatively to isotype and secondary antibody controls. (**g**) Cell survival analysis of a NBM control and eight individual primary MLL-rearranged AML patient samples upon single or combined VEGFR-2 (250 ng/ml) and MEK (1 μM) inhibition. *Significant reduction in AML cell survival relative to control and #synergistic significant reduction in AML cell survival upon combination therapy compared with both mono-therapies ($P<0.05$). (**h**) Immunoblot analysis of primary MLL-rearranged AML samples upon single or combined VEGFR-2 (250 ng/ml) and MEK (1 μM) inhibition for mTOR phosphorylation. Changes in protein phosphorylation were not due to an overall increase in protein synthesis, as shown with western blot analysis against actin.

therapy was examined in our cell line model using THP-1 and competitor HL60 both expressing VEGFR-2 on their cell membrane (Supplementary Figure 3). Short-term 48 h combination therapy reduced THP-1 cell survival more efficiently compared with single inhibitors (Figure 5b, Student's *t*-test $P<0.001$). Comparable in HL60, combination therapy decreased HL60 cell survival, but showed less pronounced effects compared with THP-1 (Figure 5b, Student's *t*-test $P<0.001$). Subsequently, short-term (24 h and 48 h) and long-term (5 days) combination therapy effects were evaluated by phospho-proteome array analysis in THP-1 (Figures 5c and d). In addition to the already present inhibition of Erk and p70S6 protein phosphorylation and increase in Akt phosphorylation as a result of MEK inhibition, short-term combination therapy reduced VEGFR-2 phosphorylation, which was even further reduced after 5 days of treatment. Recently, c-Abl was described to act downstream of VEGFR-2.[12] Short-term and long-term combination therapy also decreased the phosphorylation of downstream c-Abl. The long-term combination therapy revealed that VEGFR-2 and c-Abl phosphorylation were largely abolished. Immunoblots confirmed that combination therapy is more effective than single therapies, as the sustained mTOR phosphorylation during MEK inhibition is sufficiently blocked upon combination therapy in MLL-rearranged AML cells, which was indicated to be partly independent from Akt phosphorylation (Figures 5d and e).

To investigate whether VEGFR-2 constitutes a potential therapeutic target for primary MLL-rearranged AML, we analyzed

VEGFR-2 membrane protein expression by flow cytometry in a large cohort of pediatric MLL-rearranged AML patient samples ($n = 32$). Primary MLL-rearranged AML cells showed significantly increased VEGFR-2 membrane protein expression levels as compared with NBM and non-MLL-rearranged AML samples (Figure 5f and Supplementary Figure 4, Mann–Whitney *U*-test, $P < 0.001$ and $P = 0.038$). To evaluate whether VEGFR-2 antibody therapy could improve therapeutic sensitivity to MEK inhibition, we analyzed combination therapy effects in primary MLL-rearranged AML samples ($n = 8$). Short-term combination treatment of primary MLL-rearranged AML samples provided a stronger reduction in cell survival compared with single MEK inhibition in three out of the eight tested primary MLL-rearranged AML samples (Figure 5g). The MLL-rearranged AML samples that showed a stronger reduction in AML cell survival upon combination therapy were all RAS WT AML patient samples. Interestingly, NBM cells subjected to the same combination therapy did not show any effects upon MEK inhibition or combination therapy. Phosphorylated levels of mTOR were relatively low in primary MLL-rearranged AML, however, we found that mTOR phosphorylation was maintained mostly during MEK inhibition. Single VEGFR-2 inhibition or in addition to the MEK inhibition was sufficient to block mTOR phosphorylation in primary MLL-rearranged AML (Figure 5h). This finding suggests that combined MEK- and VEGFR-2-targeting therapy could be promising in a subset of AML represented with high MEK and mTOR phosphorylation and high VEGFR-2 membrane protein expression.

DISCUSSION

Genetic, epigenetic and cellular pathway adaptations accumulate leading to leukemic transformation and proliferation. Translocations, molecular aberrations and mutations cannot be changed; they are a given failure of the system. However, leukemic cells can be targeted through their aberrant protein signaling networks corresponding to the genetic and environmental changes that promote leukemia progression and maintenance. With the use of combined kinomic and proteomic activity profiling of primary MLL-rearranged AML samples, we obtained important insights in disease biology and unique machinery networks to develop novel potential therapeutic strategies. Signaling pathway adaptations or sustained activity of alternative escape routes upon mono-therapy can be detected using our high-throughput approach to define more rational combination therapies. The analysis of dynamic escape mechanisms allowed us to predict and test the efficacy of novel combination strategies for MLL-rearranged AML blasts.

MLL translocations fuse the common MLL N-terminus in frame, with over 60 translocation partner genes. MLL binds the DNA with high affinity to induce the transcription of MLL target genes, such as HOXA9, MEIS1, CDKs and Pbx.[13–16] In turn, a complex composed of HOX, MEIS1, TORC (mTOR complex), CBP and CREB can promote important proliferation and anti-apoptotic signals. This complex has been shown to be dependent on CREB phosphorylation, as a GSK-3 inhibitor reduced CREB phosphorylation, which consistently blocked the critical target gene expression responsible for HOX-mediated transformation in MLL-rearranged leukemia cells.[16] The CREB inhibitor KG-501 that we used in this manuscript does not target CREB phosphorylation, however, targets a surface distal to the CREB-binding groove that is required for the CREB-CBP interaction. Even though, BCL2 is a downstream target of CREB that is inhibited by KG-501, it was not found to decrease MLL-rearranged cell survival differently from NBM controls. It might be that the CREB–CBP interaction is not required to accomplish the MLL-rearranged complex of HOX, MEIS1, TORC, CBP and CREB. This might partly explain why the AML patient samples were heterogeneously responsive to KG-501.

In this study, high-throughput kinome and proteome analysis of MLL-rearranged AML patient samples revealed MLL-selective kinome and proteome activity profiles. These profiles defined proteins that might be responsible for the advantageous proliferation and survival status of MLL-rearranged AML cells. Figure 6a outlines the MLL-rearrangement protein activity profile in AML and how the balance compared with NBM is hypothesized to be disturbed. The MLL-rearranged AML profile is characterized by increased activity of the MAPK/MEK/Erk pathway and high VEGFR-2 expression in coexistence with an impaired PI3K pathway activity, as we found using kinome and proteome arrays.

Inhibition of the MAPK pathway by a MEK inhibitor reduced Erk, GSK-3 and CREB phosphorylation *in vitro* in this study. When CREB is not phosphorylated, the MLL rearrangement-mediated complex is not formed and disintegrates, which partly results in MLL-rearranged AML cell death. Nevertheless, short-term and long-term MEK inhibition proteome profiles revealed the continues activity of a survival route to outlive the initial MEK inhibition as presented in Figure 6b. Although the PI3K pathway was impaired, this pathway showed sustained activity upon MEK inhibition, and therefore, could facilitate an alternative escape route, through which MEK resistance develops. We hypothesize that the resistant pathway allows a subpopulation of AML cells to survive MEK inhibition, which under the extreme induction of VEGFR-2 and Erk phosphorylation, after MEK exhaustion could be able to resume their proliferation. Our data indicate that the MAPK pathway is mainly important for the proliferative state of the AML cells, whereas VEGFR-2 and the PI3K signaling pathway are important for the MLL-rearranged AML cell survival. The contribution of the PI3K pathway to cellular resistance was quite unexpected from the MLL-rearranged AML kinome and proteome profiles, which convincingly showed decreased activity of downstream PI3K pathway proteins.

It has been described that one-third of the MLL-rearranged AML primary samples harbor mutations in N-RAS, K-RAS or PTPN11.[17] Oncogenic lesions occur in a single RAS isoform, the remaining two isoforms are still wild type. A recent study by Young *et al.* showed that in three cancer cell models, oncogenic RAS regulates basal MAPK signaling and wild-type RAS mediates downstream signaling as a second driver of tumor cell proliferation. And importantly, oncogenic RAS negatively regulates RTK signaling. Depleting oncogenic RAS recovers the negative feedback of RTKs as well as activation of wild-type RAS signaling.[18] In our MLL-rearranged AML cell line model, the interplay of oncogenic and wild-type RAS isoforms may have an identical function in the one-third harboring RAS mutations. The mutations in RAS and PTPN11 lead to enhanced activation of the MAPK pathway that we found in MLL-rearranged AML as compared with NBM. In this manuscript, it has been shown that downstream MEK inhibition is an effective strategy to block MAPK pathway activity, nevertheless, MEK inhibition was quickly exhausted resulting in Erk activity supported by the increased activity of VEGFR-2.

The PI3K/Akt/mTOR signaling network is one of the most frequently deregulated pathways involved in the pathogenesis of cancer. This can be the result of mutational activation (for example, mutations in PI3K/AKT or RTKs), nevertheless, PI3K, Akt and mTOR are key nodes in signaling integrating input from various sources such as non-mutant overexpressed RTKs and GTPases.[19,20] In AML, high basal levels of phosphorylated Akt have been associated with a poor prognosis.[21] High steady-state levels of phosphorylated Akt, Erk and/or total protein expression levels of Erk and PKC were adverse factors for AML survival.[22] We describe that in MLL-rearranged AML the phosphorylation levels of Akt were relatively high in primary AML cells at diagnosis, whereas mTOR and p70S6k phosphorylation were found significantly lower in MLL-rearranged AML. The sustained activity of Akt and mTOR upon MEK inhibition was effectively targeted by combined MEK and VEGFR-2 inhibition therapy in MLL-rearranged AML, which are potentially important for the cell survival and proliferation in a subset of AML. These findings clearly show the

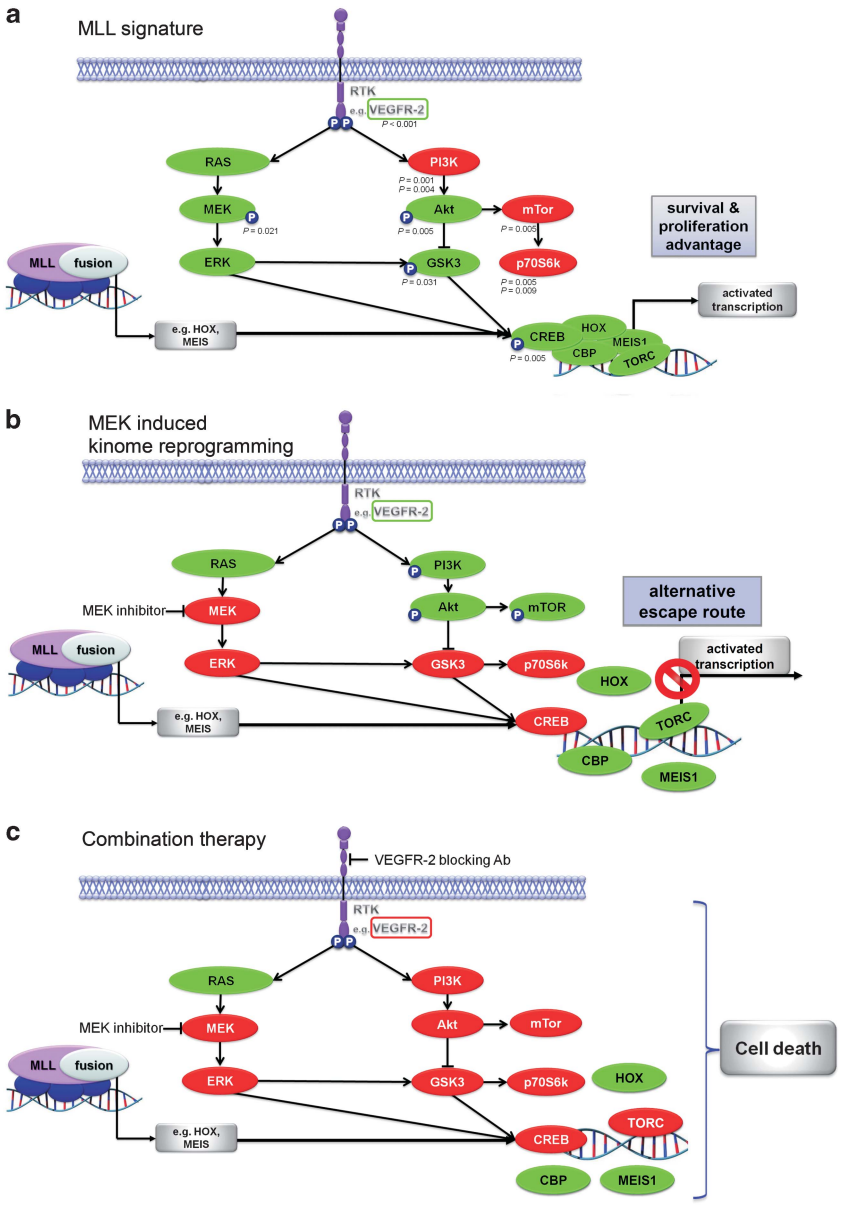

Figure 6. MLL-rearranged AML protein kinase activity profile and dynamic kinome reprogramming as a consequence of MEK inhibition. (**a**) MLL fusion proteins (on the left) induce the expression of MLL target genes. In turn, a complex can be formed that is able to drive proliferation. This complex is dependent on CREB phosphorylation mediated by Erk and GSK-3 activity, resulting in the selective MLL-rearranged AML protein activity profile. The MLL-rearranged AML profile as compared with NBM, showed a general induction of MAPK pathway proteins and a reduction of some of the PI3K pathway proteins. The proteins in red show a downregulated activity in MLL-rearranged AML as compared with NBM, whereas the green proteins represent increased protein activity. (**b**) Short-term MEK inhibition induced Akt phosphorylation, which in turn could have led to the sustained activation of mTOR. Erk was found to be re-activated after long-term MEK that could have been the net result of induced VEGFR-2 phosphorylation from a feedback mechanism and MEK inhibition exhaustion. (**c**) Combined MEK and VEGFR-2 inhibition resulted in a inhibition of the MEK signaling pathway and VEGFR-2/mTOR signaling pathway in a subset of MLL-rearranged AML samples.

complexity and redundancy of signaling networks with feedback mechanisms and escape routes. The use of high-throughput measurements provided insights in the complexity of the PI3K pathway in MLL-rearranged AML.

To control dynamic kinome reprogramming, we combined MEK inhibition with RTK inhibition of VEGFR-2. In Figure 6c it is shown that upon combination therapy, not only the proliferative signals by activating the CREB complex are blocked, but also the escape mechanism of the PI3K/Akt/mTOR signaling pathway, leading to a reduction of the MLL-rearranged AML cells in a subset of AML samples. Using this methodological approach, enabled us to develop a novel combination therapy for MLL-rearranged AML by targeting the signaling pathway adaptations. However, even though anti-VEGFR-2 therapy in addition to MEK inhibition limited cellular recovery from MEK inhibition via decreased mTOR activity, especially in primary MLL-rearranged AML samples a third target would be required to strengthened this therapeutic approach further.

In conclusion, our results showed that combining kinomic and proteomic profiling is a valuable tool to generate a global view of aberrantly active signaling networks in MLL-rearranged AML. Our systematic approach provides putative targets for novel

combination therapies, which encouraged VEGFR-2 and MEK combination therapy as a first step using this identification approach. This strategy is applicable to many cancer subgroups for which the search for more sophisticated therapeutic innovations continues.

CONFLICT OF INTEREST

The authors declare no conflict of interest.

ACKNOWLEDGEMENTS

RAS pathway mutations were obtained from MWJ Fornerod, MM van den Heuvel-Eibrink and CM Zwaan from the Department of Pediatric Oncology/Hematology, Erasmus MC—Sophia Children's Hospital, Rotterdam, Netherlands. We thank Imclone for their generous supply of VEGFR-2 antibody IMC1121b. We also thank the patients who donated leukemia specimens and also physician assistants, nurse practitioners and fellows who acquired specimens. KRK was supported by a grant from the Foundation for Pediatric Oncology Groningen, The Netherlands (SKOG). The kinome data collection was supported by a grant from the Foundation KiKa, Amstelveen (AtE, HM and ESJMdB).

AUTHOR CONTRIBUTIONS

KRK performed research, collected data, analyzed data and wrote the paper. AtE performed peptide array and background subtraction. HM performed statistical testing of peptide array results. SHD guided performing the peptide arrays. FJGS performed research and collected data. VdH contributed samples. MPP designed peptide arrays. VG performed quantile normalization and supervised peptide array analysis. ESJMdB designed research, analyzed data, supervised and wrote the paper.

REFERENCES

1 Chapuis N, Park S, Leotoing L, Tamburini J, Verdier F, Bardet V *et al.* IkappaB kinase overcomes PI3K/Akt and ERK/MAPK to control FOXO3a activity in acute myeloid leukemia. *Blood* 2010; **116**: 4240–4250.
2 Chen E, Staudt LM, Green AR. Janus kinase deregulation in leukemia and lymphoma. *Immunity* 2012; **36**: 529–541.
3 Tamburini J, Elie C, Bardet V, Chapuis N, Park S, Broet P *et al.* Constitutive phosphoinositide 3-kinase/Akt activation represents a favorable prognostic factor in *de novo* acute myelogenous leukemia patients. *Blood* 2007; **110**: 1025–1028.
4 Ter Elst A, Diks SH, Kampen KR, Hoogerbrugge PM, Ruijtenbeek R, Boender PJ *et al.* Identification of new possible targets for leukemia treatment by kinase activity profiling. *Leuk Lymphoma* 2011; **52**: 122–130.
5 Kornblau SM, Coombes KR. Use of reverse phase protein microarrays to study protein expression in leukemia: technical and methodological lessons learned. *Methods Mol Biol* 2011; **785**: 141–155.
6 Tibes R, Qiu Y, Lu Y, Hennessy B, Andreeff M, Mills GB *et al.* Reverse phase protein array: validation of a novel proteomic technology and utility for analysis of primary leukemia specimens and hematopoietic stem cells. *Mol Cancer Ther* 2006; **5**: 2512–2521.
7 Kantarjian H, Sawyers C, Hochhaus A, Guilhot F, Schiffer C, Gambacorti-Passerini C *et al.* Hematologic and cytogenetic responses to imatinib mesylate in chronic myelogenous leukemia. *N Engl J Med* 2002; **346**: 645–652.
8 Duncan JS, Whittle MC, Nakamura K, Abell AN, Midland AA, Zawistowski JS *et al.* Dynamic reprogramming of the kinome in response to targeted MEK inhibition in triple-negative breast cancer. *Cell* 2012; **149**: 307–321.
9 Dokter WH, Tuyt L, Sierdsema SJ, Esselink MT, Vellenga E. The spontaneous expression of interleukin-1 beta and interleukin-6 is associated with spontaneous expression of AP-1 and NF-kappa B transcription factor in acute myeloblastic leukemia cells. *Leukemia* 1995; **9**: 425–432.
10 Lunghi P, Tabilio A, Dall'Aglio PP, Ridolo E, Carlo-Stella C, Pelicci PG *et al.* Downmodulation of ERK activity inhibits the proliferation and induces the apoptosis of primary acute myelogenous leukemia blasts. *Leukemia* 2003; **17**: 1783–1793.
11 Odenike O, Curran E, Iyengar N, Popplewell L, Kirschbaum M, Erba HP *et al.* Phase II Study of the Oral MEK Inhibitor AZD6244 in Advanced Acute Myeloid Leukemia (AML). *Blood* 2009; **114**: 821–822.
12 Anselmi F, Orlandini M, Rocchigiani M, De CC, Salameh A, Lentucci C *et al.* c-ABL modulates MAP kinases activation downstream of VEGFR-2 signaling by direct phosphorylation of the adaptor proteins GRB2 and NCK1. *Angiogenesis* 2012; **15**: 187–197.
13 Cierpicki T, Risner LE, Grembecka J, Lukasik SM, Popovic R, Omonkowska M *et al.* Structure of the MLL CXXC domain-DNA complex and its functional role in MLL-AF9 leukemia. *Nat Struct Mol Biol* 2010; **17**: 62–68.
14 Faber J, Krivtsov AV, Stubbs MC, Wright R, Davis TN, Heuvel-Eibrink M *et al.* HOXA9 is required for survival in human MLL-rearranged acute leukemias. *Blood* 2009; **113**: 2375–2385.
15 Liedtke M, Cleary ML. Therapeutic targeting of MLL. *Blood* 2009; **113**: 6061–6068.
16 Wang Z, Iwasaki M, Ficara F, Lin C, Matheny C, Wong SH *et al.* GSK-3 promotes conditional association of CREB and its coactivators with MEIS1 to facilitate HOX-mediated transcription and oncogenesis. *Cancer Cell* 2010; **17**: 597–608.
17 Balgobind BV, Hollink IH, Arentsen-Peters ST, Zimmermann M, Harbott J, Beverloo HB *et al.* Integrative analysis of type-I and type-II aberrations underscores the genetic heterogeneity of pediatric acute myeloid leukemia. *Haematologica* 2011; **96**: 1478–1487.
18 Young A, Lou D, McCormick F. Oncogenic and wild-type Ras play divergent roles in the regulation of mitogen-activated protein kinase signaling. *Cancer Discov* 2013; **3**: 112–123.
19 Rodrik-Outmezguine VS, Chandarlapaty S, Pagano NC, Poulikakos PI, Scaltriti M, Moskatel E *et al.* mTOR kinase inhibition causes feedback-dependent biphasic regulation of AKT signaling. *Cancer Discov* 2011; **1**: 248–259.
20 Wilson TR, Fridlyand J, Yan Y, Penuel E, Burton L, Chan E *et al.* Widespread potential for growth-factor-driven resistance to anticancer kinase inhibitors. *Nature* 2012; **487**: 505–509.
21 Gallay N, Dos SC, Cuzin L, Bousquet M, Simmonet GV, Chaussade C *et al.* The level of AKT phosphorylation on threonine 308 but not on serine 473 is associated with high-risk cytogenetics and predicts poor overall survival in acute myeloid leukaemia. *Leukemia* 2009; **23**: 1029–1038.
22 Kornblau SM, Womble M, Qiu YH, Jackson CE, Chen W, Konopleva M *et al.* Simultaneous activation of multiple signal transduction pathways confers poor prognosis in acute myelogenous leukemia. *Blood* 2006; **108**: 2358–2365.

Supplementary Information accompanies this paper on the Leukemia website (http://www.nature.com/leu)